

Modeling of Local BEAM Structure for Evaluation of MMOD Impacts to Support Development of a Health Monitoring System

Karen H. Lyle
Langley Research Center, Hampton, Virginia

Gregory J. Vassilakos
Analytical Mechanics Associates, Hampton Virginia

NASA STI Program . . . in Profile

Since its founding, NASA has been dedicated to the advancement of aeronautics and space science. The NASA scientific and technical information (STI) program plays a key part in helping NASA maintain this important role.

The NASA STI program operates under the auspices of the Agency Chief Information Officer. It collects, organizes, provides for archiving, and disseminates NASA's STI. The NASA STI program provides access to the NTRS Registered and its public interface, the NASA Technical Reports Server, thus providing one of the largest collections of aeronautical and space science STI in the world. Results are published in both non-NASA channels and by NASA in the NASA STI Report Series, which includes the following report types:

- **TECHNICAL PUBLICATION.** Reports of completed research or a major significant phase of research that present the results of NASA Programs and include extensive data or theoretical analysis. Includes compilations of significant scientific and technical data and information deemed to be of continuing reference value. NASA counter-part of peer-reviewed formal professional papers but has less stringent limitations on manuscript length and extent of graphic presentations.
- **TECHNICAL MEMORANDUM.** Scientific and technical findings that are preliminary or of specialized interest, e.g., quick release reports, working papers, and bibliographies that contain minimal annotation. Does not contain extensive analysis.
- **CONTRACTOR REPORT.** Scientific and technical findings by NASA-sponsored contractors and grantees.

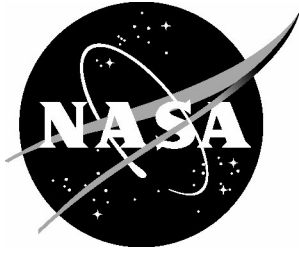
- **CONFERENCE PUBLICATION.** Collected papers from scientific and technical conferences, symposia, seminars, or other meetings sponsored or co-sponsored by NASA.
- **SPECIAL PUBLICATION.** Scientific, technical, or historical information from NASA programs, projects, and missions, often concerned with subjects having substantial public interest.
- **TECHNICAL TRANSLATION.** English-language translations of foreign scientific and technical material pertinent to NASA's mission.

Specialized services also include organizing and publishing research results, distributing specialized research announcements and feeds, providing information desk and personal search support, and enabling data exchange services.

For more information about the NASA STI program, see the following:

- Access the NASA STI program home page at <http://www.sti.nasa.gov>
- E-mail your question to help@sti.nasa.gov
- Phone the NASA STI Information Desk at 757-864-9658
- Write to:
NASA STI Information Desk
Mail Stop 148
NASA Langley Research Center
Hampton, VA 23681-2199

NASA/TM-2015-218985



Modeling of Local BEAM Structure for Evaluation of MMOD Impacts to Support Development of a Health Monitoring System

Karen H. Lyle

Langley Research Center, Hampton, Virginia

Gregory J. Vassilakos

Analytical Mechanics Associates, Hampton Virginia

National Aeronautics and
Space Administration

Langley Research Center
Hampton, Virginia 23681-2199

November 2015

The use of trademarks or names of manufacturers in this report is for accurate reporting and does not constitute an official endorsement, either expressed or implied, of such products or manufacturers by the National Aeronautics and Space Administration.

Available from:

NASA STI Program / Mail Stop 148
NASA Langley Research Center
Hampton, VA 23681-2199
Fax: 757-864-6500

Abstract

This report summarizes initial modeling of the local response of the Bigelow Expandable Activity Module (BEAM) to micrometeorite and orbital debris (MMOD) impacts using a structural, non-linear, transient dynamic finite element code. Complementary test results for a local BEAM structure are presented for both hammer and projectile impacts. Review of these data provided guidance for the transient dynamic model development. The local model is intended to support predictions using the global BEAM model, described in a companion report. Two types of local models were developed. One mimics the simplified Soft-Goods (fabric envelop) part of the BEAM NASTRAN model delivered by the project. The second investigates through-the-thickness modeling challenges for MMOD-type impacts. Both the testing and the analysis summaries contain lessons learned and areas for future efforts.

1. Introduction

Micrometeorite and Orbital Debris (MMOD) impacts are a common threat for human and robotic spacecraft traveling in low earth orbit, see Ref [1]. Design approaches for protecting spacecraft against MMOD impacts that degrade the performance or cause catastrophic destruction have been studied extensively, see Ref. [2]. Flexible spacecraft structural components present a particularly challenging structure to protect. For human-rated space habitats, a demonstration module has been fabricated utilizing the design approach documented in a US Patent, see Refs. [3 and 4]. This demonstration module has been designated the Bigelow Expandable Activity Module (BEAM), which will be attached to the International Space Station (ISS) as illustrated in Figure 1, see Ref. [5].

A number of numerical methods and associated hardware for damage detection for MMOD type impacts have been documented in the literature, see Ref. [6-12]. The simulations presented in this report have been developed to align with the Distributed Impact Detection System (DIDS) deployment testing on BEAM, see Refs. [13-15]. DIDS is an array of accelerometers, connected to a processor that can be used to determine the location of MMOD impacts, as shown notionally in Figure 2.

Historically, hypervelocity testing has been conducted to determine MMOD impact performance. Hypervelocity testing is very expensive and is only feasible for shields in the later phases of design. Therefore, advancement of analytical methods is important to develop protection against MMOD impacts for novel structures in the early trade study and design phases. The purpose of this report is to document progress made in developing spacecraft structural modeling of MMOD impact and relevance to active impact detection systems. The focus here is the development of a

model suitable to understand MMOD impacts on soft-goods structures such as the BEAM. A companion report highlights global BEAM modeling behavior.

2. Component testing

Impact testing on a 38 x 38 cm MMOD shield sample supported on a 67 x 67 cm restraint-layer framework was conducted, see Refs. [16, 17]. A photograph of the test article is shown in Figure 3, with a schematic cross-section shown in Figure 4. This test configuration was used for both the hammer and the projectile testing. The test articles had foam spacers that were shaped like picture frames or cored with cylindrical through-the-thickness holes, see Figure 5. For all of the hammer testing, the foam spacers were shaped like picture frames. For most of the projectile tests, the foam was also picture-frame shaped. To facilitate comparison with previous vendor-supported projectile tests, a few projectile impacts with the cored-foam spacers were tested. The picture-frame shaped test configuration is the baseline and cored-foam test configuration will be specified as needed. From a simulation perspective, the details of the restraint layer are the most relevant, as the DIDS accelerometers will be attached to this layer.

Placement of the accelerometers is shown in Figure 6. The instrumentation consisted of paired accelerometers at each location. Specifically, DIDS accelerometers were located as close as possible with Facility accelerometers. The Facility accelerometers provided continuous data. The DIDS accelerometers trigger only when a signal of a certain magnitude is detected. Unfortunately for projectile impacts, the location of the DIDS sensors on the restraint layer will likely result in missing some of the initial data as the DIDS wake up and start recording data. Nonetheless, the testing provides a great deal of information about how the signals will propagate through the layers and the physics of the double strap responses.

2.1 Hammer impact testing

A series of 15 instrumented hammer tests were performed with impact locations on the restraint layer, the exterior shield surface, and the sample frame. At each site, the responses from three hammer impacts were recorded. The data in the figures are for the Facility accelerometers. These tests were important to the modeling because of their excitation control and the ability to directly impact locations not possible to access during projectile testing. For example, hammer impacts were performed directly on the restraint layer.

The restraint-layer acceleration responses to three hammer impacts on shield Layer 1 are shown in Figure 7. This set of measurements approximates an MMOD impact that produces no damage to the outer most shield layer. The data confirm the

transmission of a hammer impact on the front of shield Layer 1 to the accelerometers on the back of the restraint layer. (corresponding front and back locations on the restraint layer have been plotted on the same graph). The front-to-back accelerometers exhibit an equal and opposite behavior. The light tension of Layer 1 generated a rather “soft” response rather than the sharp impulse typically seen in hammer testing. The overlay of the responses for the three impacts provides confidence in the repeatability of the structural response to similar impacts.

In contrast, the hammer impact on the tensioned restraint layer results in a much sharper impact of approximately twice the amplitude, see Figure 8. Again, the responses for the three hammer excitations are generally repeatable and front-to-back accelerometers show an equal-and-opposite response.

2.2 Projectile impacts

For the projectile tests, nine tests were performed with projectiles of varying size, material, and impact velocity. In addition, prior to these tests, the vendor conducted 15 projectile tests, with projectiles of varying sizes, impact angles, and impact velocities. Although descriptions of the damage were provided for the vendor tests, no acceleration measurements were acquired. For all of the vendor conducted impacts, the foam picture-frame spacers were replaced with a cored-foam spacer.

Figure 9 provides a comparison of accelerations for projectile impacts with two foam spacer configurations. Only the back restraint layer accelerometers have been shown, because these locations represent the on-orbit BEAM application. Time $t=0$ has been established by time shifting the measurements. For the set of data in the top row (HITF 14103), the mass is 0.133g, impact angle=45-deg., impact velocity=5.42 km/s, and the foam spacer is the “cored” configuration. For the bottom row (HITF 14105), the mass is 0.0138 g, impact angle=30-deg, impact velocity=3.10 km/s, and the foam space is the “picture-frame” configuration. Both tests produced similar damage in that the first and second layers were damaged, with no damage to the 3rd and final layer. However, the normal kinetic energy at impact is an order of magnitude different. The responses for test HITF14105 are an order of magnitude less than those for HITF 14103, which correlates to the approximate difference in impact kinetic energy. Both configurations of the foam spacer provide a mechanism to transfer energy to the restraint-layer.

A collection of the normal kinetic energy versus projectile mass for all tests are shown in Figure 10. A line fit through the pass data points has been computed to approximate a threshold. The pass conditions were identified by the project as those tests where the restraint layer remained undamaged. Impacts above this line are

presumed to fail MMOD protection, as evidenced by the failure points lying just above the line.

The comparison of responses for two similar tests, which were near the pass-fail threshold are presented, see Figure 11. Here, both the impact conditions, the foam spacer configuration and the damage, are similar. In case (HITF 14107B), the mass=0.312g, impact angle=45-deg., and impact velocity=6.83 km/s. For case (HITF14108), the mass=0.120g, impact angle=30-deg., and impact velocity=7.00 km/sec. The similarity in the restraint-layer responses for the two tests provides confidence in the ability to eventually utilize such test data to validate the models.

2.3 Testing Summary

It should be noted that potential differences between the test samples and the on-orbit BEAM structure are: 1) tension in the various layers; and 2) interlayer foam spacer configuration. In spite of these differences, significant insights proved useful to support model development:

1. Impacts on the outer model layer will propagate to the restraint layer through the foam spacers. The details of the transmissions could depend on the geometry of the interlayer foam spacers.
2. The two layers of restraint-layer straps act as a single layer as noted by the equal and opposite responses for corresponding front-to-back accelerometers pairs.
3. The repeatability of the responses is good as demonstrated by the similarity of responses for the three hammer impacts at each location.
4. For the test article, the wave propagation in the restraint layer is approximately 200 m/s, with a fundamental vibration frequency of 110 Hz. The component restraint layer tension is less than that for the on-orbit configuration because of the limited capability for tensioning straps in the lab.

3.0 Component model

Two component models were developed for investigations of the ability of LS-DYNA®, see Ref. [18], to capture the basic physics of the BEAM panel tests. These were referred to as: 1) the Simple Model and 2) the Layer Model. To date, the simulations were intended to represent non-penetrating hammer impacts that cause no damage to the material.

3.1 Simple Model

The Simple Model consisted of a square sheet of shell elements 67.31 cm (26.5 in.) on a side. The model is illustrated in Figure 12. The model properties are provided in Table 1. As the purpose of the model was to investigate the ability to capture

basic physics of wave propagation through a membrane rather than to match particular test results, the properties used were approximate and do not match material properties used for later investigations.

The material was modeled as a fabric (*MAT_FABRIC), which has no compressive stiffness or bending stiffness. For solution stability, a small amount of compressive stiffness was provided based on the definition of a fabric liner. The liner was assigned the same properties as the fabric, but the thickness was just 2% of the fabric thickness. The liner was assigned a damping factor of 0.05 (5% critical damping).

For the simulations, the panel was tensioned via a thermal load and then a short duration force pulse representing an MMOD impact was applied at the center. The load histories are described in Figure 13. The tensile preload in the panel was established by imposing a temperature change of -11.5 degrees ramped over 0.1 seconds. The force at the center of the panel was a triangular spike with a duration of 0.002 seconds and a peak amplitude of 10 dynes that begins at the end of the 0.1 second preload ramp.

The primary characteristic of interest in the model was the natural frequency. This was determined by performing a fast Fourier transform (FFT) of the velocity history. The velocity histories of four nodes of the baseline model are illustrated in Figure 14. A sample plot of the FFT of the baseline responses is shown in Figure 15. The natural frequency stands out at 628 Hz and changes in a manner consistent with the theory. It has been recognized that this is substantially higher than the test value. However, this difference in vibration frequency will not affect the conclusions resulting from the parameter studies in this section.

Two parameter studies were performed with the model. In the first, the elastic modulus was varied. The thermal expansion coefficient was varied simultaneously to keep the preload tension constant. The variants featured the baseline elastic modulus multiplied by 0.125, 0.25, 0.5, 1, 2, 4, and 8, see Figure 16.

For the second parameter study, the tension was varied by adjusting the temperature change while holding the elastic modulus and thermal expansion coefficient constant. The variants featured the baseline temperature change multiplied by 0.5, 1, and 2, see Figure 17.

These results are consistent with theory. For a guitar string of a given length, the frequency is proportional to the square root of the tension in the string divided by

the mass per unit length. Figure 17 shows such a relationship for the panel membrane. The explanation for the insensitivity to the elastic modulus is that small deflections do not significantly change the tension, so the tension does not significantly deviate from the pretension. As the panel deflects out of plane, the deflection is resisted by the out-of-plane component of the pretension. This is illustrated in Figure 18.

3.2 Layer Model

The Layer Model featured outer, middle and base layers separated by foam “picture frames”. The outer and middle layers were carbon. The base layer represented a carbon sheet and a Kevlar sheet. The Kevlar sheet, representing the restraint-layer, extended beyond the foam picture frames to restraints at the approximate location of the interface with the steel frame and hardware used to apply pretension. The model is illustrated in Figure 19, with model properties provided in Table 2.

For all of the *MAT_FABRIC material models, a liner was defined that provided a small amount of compressive stiffness to help stabilize the response. The liner had the same elastic modulus and Poisson’s ratio as the fabric. The liner thickness was specified as 2% of the fabric thickness and the liner damping factor was specified as 0.05 (5% of critical damping).

The base layer was tensioned via a thermal expansion coefficient and temperature change. The temperature change was ramped over the first 0.1 seconds of the simulation as illustrated in Figure 20. The preload was set to provide a tension of $2.67\text{E}8$ dynes (600 lbs) along the edges based on a total edge length of 55.88 cm (22 inches) and a single layer of material with a thickness of 0.254 cm (0.1 inches), see Figure 21.

The impactor was modeled as a single brick element with a base 2 cm x 2 cm, a height of 10 cm, and a mass of 313 grams. Surface-to-surface contact was defined between the impactor and the outer layer with the contact stiffness based on a factor of 0.01 applied to the limiting stiffness for solution stability based on time step size and nodal mass. The impactor was given an initial velocity of 100 cm/sec and the initial position was adjusted so that impact with the outer layer occurred at 0.1 seconds.

Histories of the resultant accelerations at the center of each panel layer are shown in Figure 22. In the close-up image, it can be readily discerned that the response at the base layer is approximately $1/100^{\text{th}}$ the response at the outer layer and that the lag time for the response to reach the base layer is approximately 0.003 seconds.

3.3 Modeling Summary

The following is a summary of results from exercising of the LS-DYNA code for impacts on the local-BEAM models.

1. The panel response is primarily a function of the mass per unit area and the tension in the membrane. The response is relatively insensitive to material properties such as elastic modulus.
2. LS-DYNA® using Lagrangian finite elements is capable of capturing the basic physics of the response to a non-penetrating impact.
3. Expansion of the through-the-thickness local modeling approach to a global-model is likely possible given knowledge of the foam spacer configuration; however, this would greatly increase model size and run time.

A conventional finite element model will not capture the phase-change and subsequent transition of the projectile and splatter as the projectile penetrates layers. Penetrating impacts would presumably require a highly localized Smooth Particle Hydrodynamics (SPH) approach. Feasibility of extension of the dense SPH local-model to a global model is not known.

4. Concluding remarks

This report summarizes initial modeling of the local response of the Bigelow Expandable Activity Module (BEAM) to micrometeorite and orbital debris (MMOD) impacts using a structural, non-linear, transient dynamic finite element code. Complementary test results for a local BEAM structure are presented for both hammer and projectile impacts. Review of these data provided guidance for the transient dynamic model development. The local model is intended for eventual inclusion in the global BEAM model described in a companion report. Primary highlights include:

1. Impacts on the outer model layer will propagate to the restraint layer through the foam spacers. The details of the transmissions will depend on the geometry of the interlayer foam spacers.
2. The restraint-layer frequency response is primarily a function of the mass per unit area and the tension in the membrane. The frequency response is relatively insensitive to material properties such as elastic modulus.
3. LS-DYNA® using Lagrangian finite elements is capable of capturing the basic physics of the response to a non-penetrating impact.
4. The feasibility of incorporating non-conventional finite element modeling approaches, such as SPH, to support global predictions has yet to be determined. An alternative approach could utilize the impulse predicted by the detailed local model on the restraint layer as input to a simpler global model.

5. References

1. Anderson, B. M.(Editor): Natural Orbital Environment Guidelines for Use in Aerospace Vehicle Development. NASA TM-1994-4527, June 1994.
2. Christiansen, E. L., et al: Handbook for Designing MMOD Protection. NASA TM-2009-214785, June 2009.
3. Bigelow, Orbital Debris Shield, US Patent 7,2004460 B2, April 2007.
4. Bigelow, Orbital Debris Shield, US Patent Application Publication, US2005/0284986 A1. December 2005.
5. Website: http://en.wikipedia.org/wiki/Bigelow_Expandable_Activity_Module).
6. Chintalapudi, et al: Structural Damage Detection and Localization Using NETSHM. 2006.
7. Welty, N., et al: Computational Methodology to Predict Satellite System-Level Effects from Impacts of Untrackable Space Debris. 62nd International Astronautical Congress, Cape Town, ZA, 2011.
8. Iyer, K. A. , et al: Use of Hydrocode Modeling to Develop Advanced MMOD Shielding Designs. IEEE, 2012.
9. Shafer, F. and Janovsky, R.: Impact Sensor Network for Detection of Hypervelocity Impacts on Spacecraft. ACTA Astronautica Vol 61, 2007, pp. 901-911.
10. Melkonyan, A.; Akopian, D.; and Chen C. L. P.: A Sensor Placement Measure for Impact Detection in Structural Health Monitoring. IEEE International Conference on Systems, Man, and Cybernetics, San Antonio TX October 2009.
11. Pavarin, D. et al: Acceleration Fields Induced by Hypervelocity Impacts on Spacecraft Structures. International Journal of Impact Engineering. Vol 33, 2006, pp. 580-591.
12. Inter-Agency Space Debris Coordination Committee: Sensor Systems to Detect Impacts on Spacecraft. IADC-08-03. Version 2.1. April 2013.
13. Tian, J.; and Madaras, E. I.: An Amplitude-Based Estimation Method for International Space Station (ISS) Leak Detection and Localization Using Acoustic Sensor Networks, NASA TM-2009-215948. November 2009.
14. Wilson, W. C.; Coffey, N. C.; and Madaras, E. I.: Leak Detection and Location Technology Assessment for Aerospace Applications. NASA 2008-215347. September 2008.
15. Prosser, W. H.; and Madaras, E. I.: Distributed Impact Detector System (DIDS) Health Monitoring System Evaluation. NASA TM-2010-216694/NASA NESC-RP-07-035, May 2010.

16. Hong, T.; Hafermalz, S.; Wells, N.; and Madaras, E.: ISS BEAM MMOD Distributed Impact Sensor System Hypervelocity Impact Test: Initial Evaluation of DIDS Hardware. Internal Report, 2014
17. Christiansen, E.; Lear, D.; Madaras, E.; Lyons, F.: ISS BEAM MMOD Impact Sensor System Hypervelocity Impact Testing. Internal Report, 2014.
18. *LS-DYNA Keyword User's Manual*, Version 971, July 27, 2012 (revision: 1617).

Table 1. Simple Model Properties

Parameter	Dimension
Edge Length	67.31 cm
Thickness	0.5 cm
Mass Density	0.373 g/cm ³
Baseline Elastic Modulus	1.00E9 dyne/cm ²
Poisson's Ratio	0.3
Thermal Expansion Coef.	1.E-3 strain/deg
Temp Change	-11.5 ⁰
Thermal Stress	1.64E7 dyne/cm ²
Tension / Unit Edge Length	8.20E6 dyne/cm

Table 2. Layered Model Properties

Layer	Thickness (cm)	Element Formulation	E (dyne/cm ²)	ρ (gram/cm ³)	ν	α (deg ⁻¹)	Material Model
Outer Layer	0.4877	5 (Membrane)	4.14E11	0.695	0.3	0.	*MAT_FABRIC
Upper Foam	6.35	2 (Fully- Integrated)	6.30E6	0.021	0.05	0.	*MAT_ELASTIC
Middle Layer	0.2438	5 (Membrane)	4.14E11	0.695	0.3	0.	*MAT_FABRIC
Lower Foam	6.35	2 (Fully- Integrated)	6.30E6	0.021	0.05	0.	*MAT_ELASTIC
Base Layer*	0.254	5 (Membrane)	8.963E10	0.7343	0.3	0.001**	*MAT_FABRIC

* Base layer features nonstructural mass = 0.1695 g/cm inside foam boundary to represent lower fabric panel of Shield Layer.

** Apply temperature change of -6.69E-2 degrees to achieve base layer preload.



Figure 1. Graphic representation of BEAM attached to ISS.

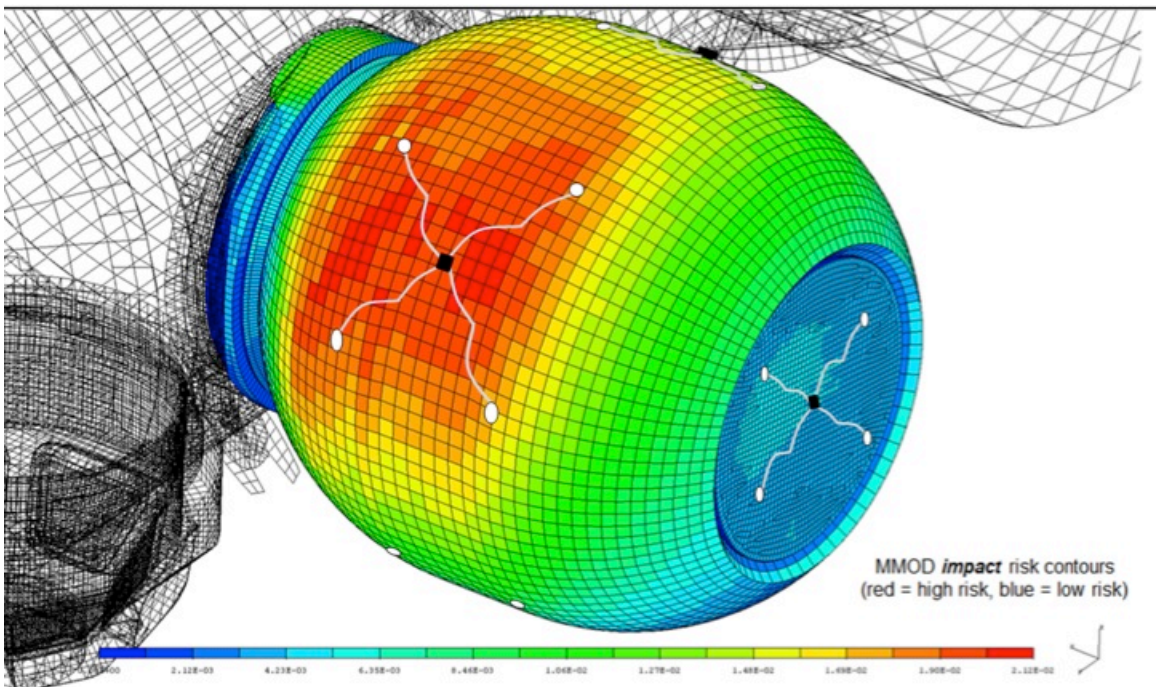


Figure 2. Illustration of DIDS sensors on-orbit.

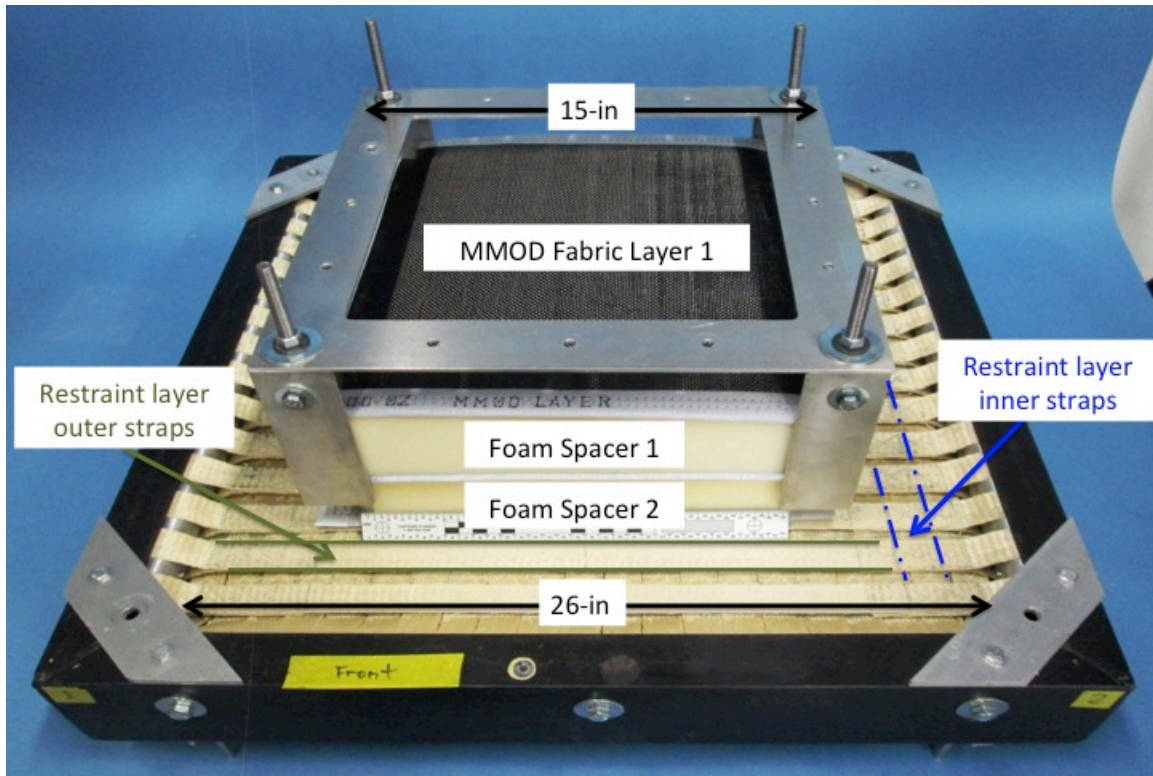


Figure 3. Photograph of component test article.

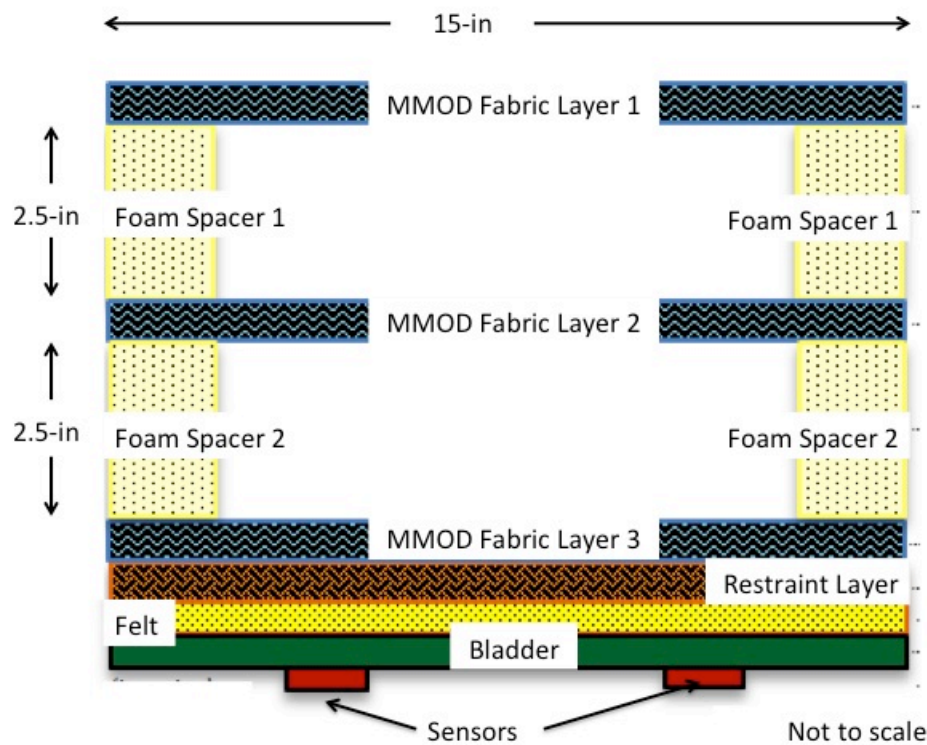


Figure 4. Through-the-thickness schematic of component test article.

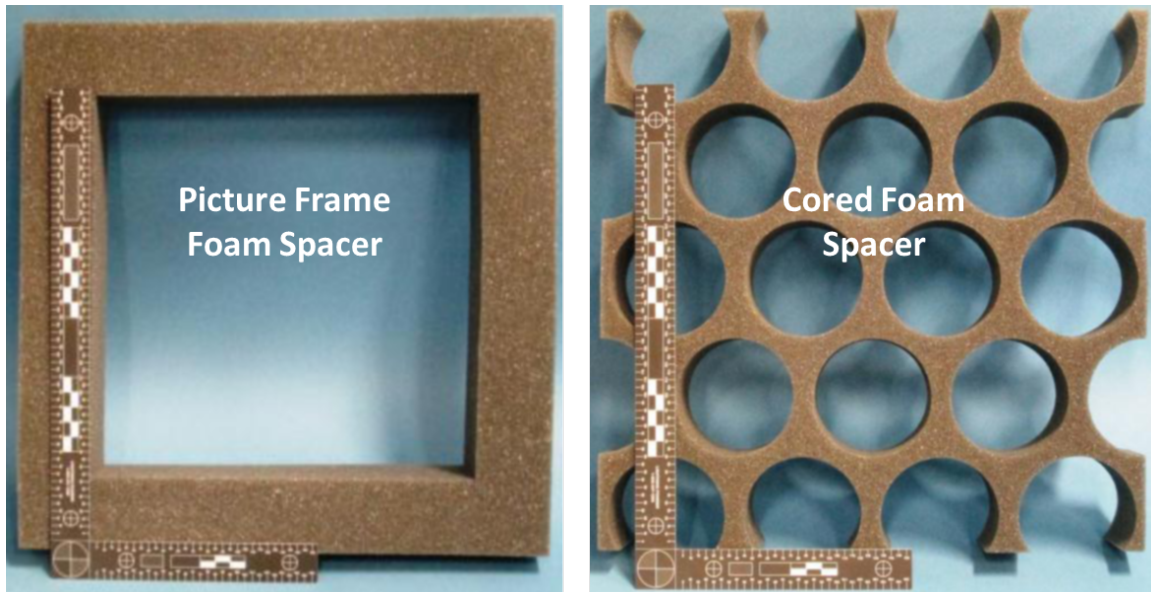


Figure 5. Picture frame and cored foam spacer configurations.

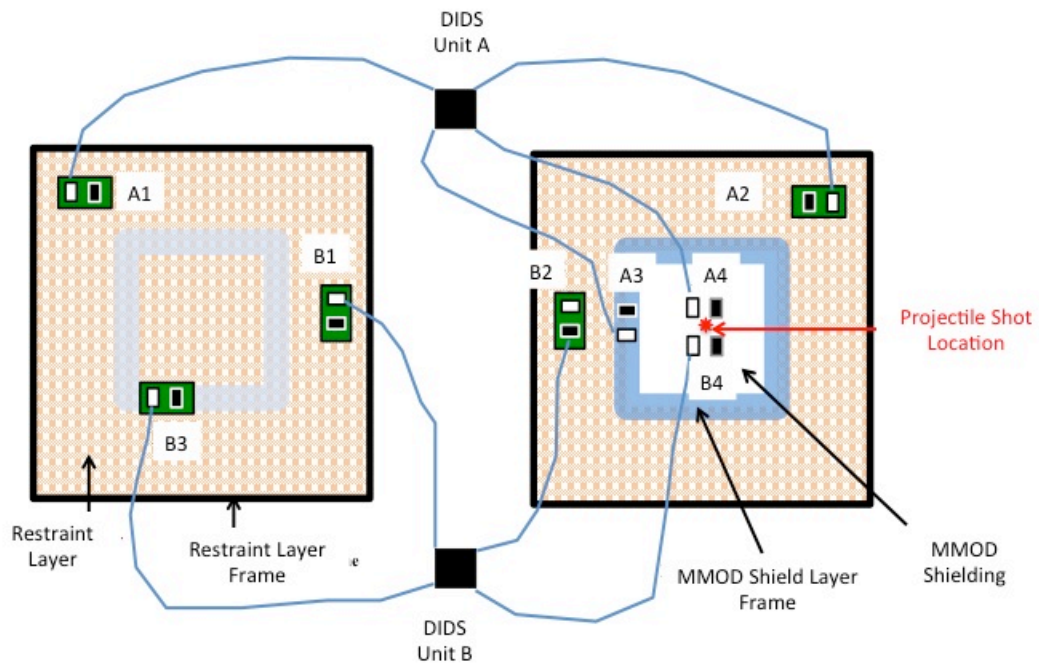


Figure 6. Diagram of DIDS and Facility accelerometer locations, denoted by side-by-side white and green rectangles, respectively.

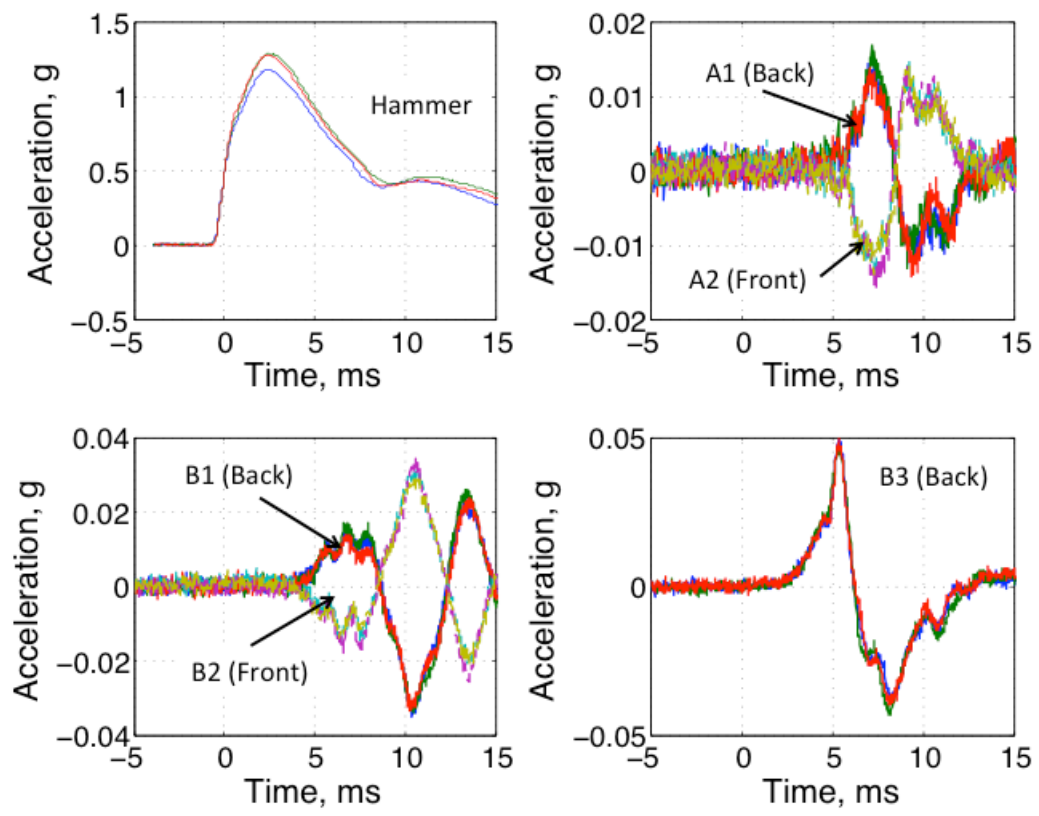


Figure 7. Restraint layer responses to impact on target front.

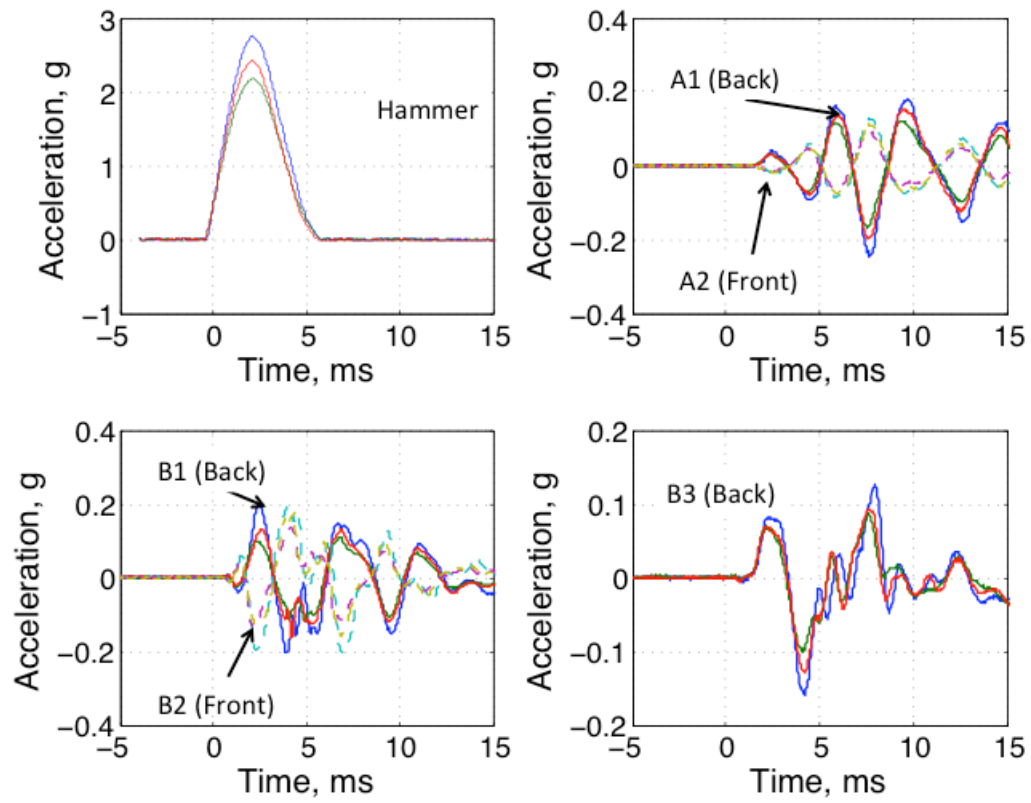


Figure 8. Restraint layer responses to impact on restraint layer front, hammer site 8.

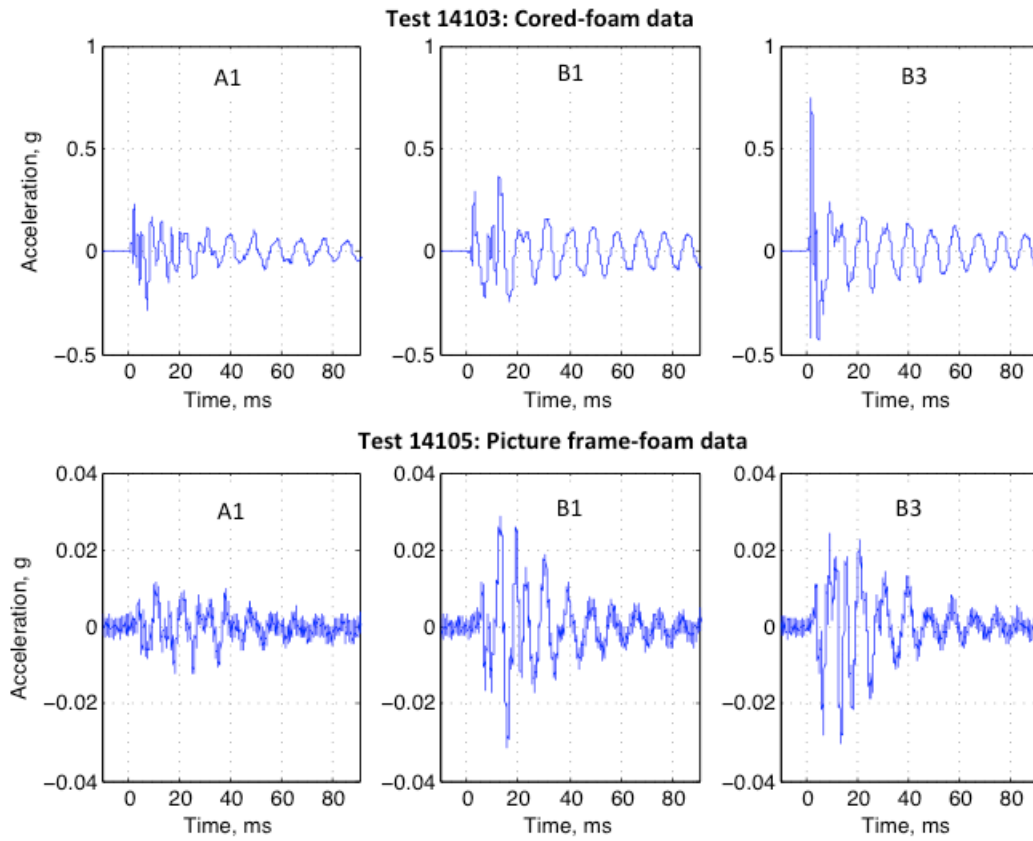


Figure 9. Restraint layer responses due to impacts that damage layers 1 and 2.

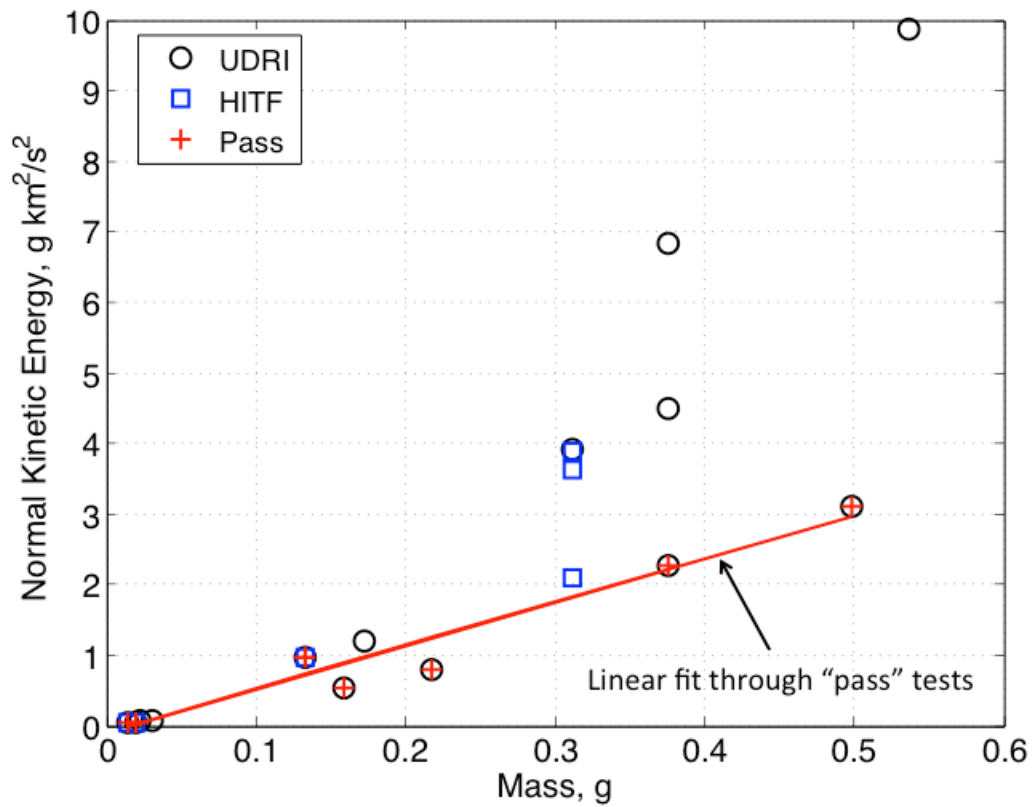


Figure 10. Damage assessments for all impacts. (HITF: Hypervelocity Impact Test Facility; UDRI: University of Dayton Research Institute)

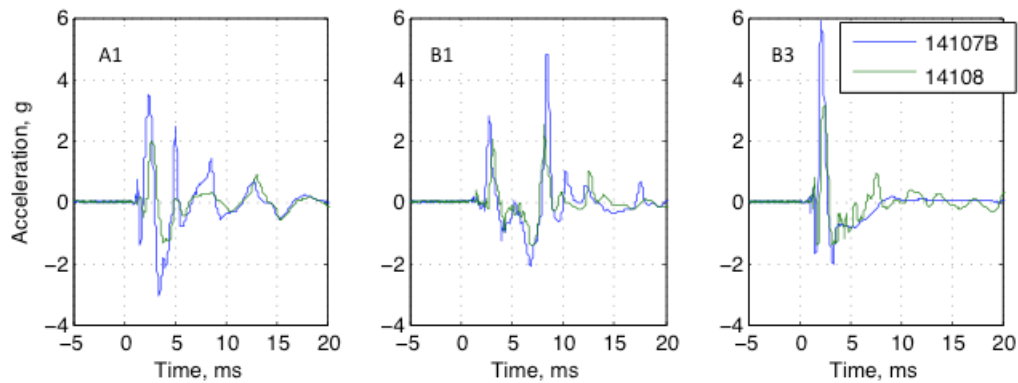


Figure 11. Restraint layer responses due to impacts that penetrate all layers.

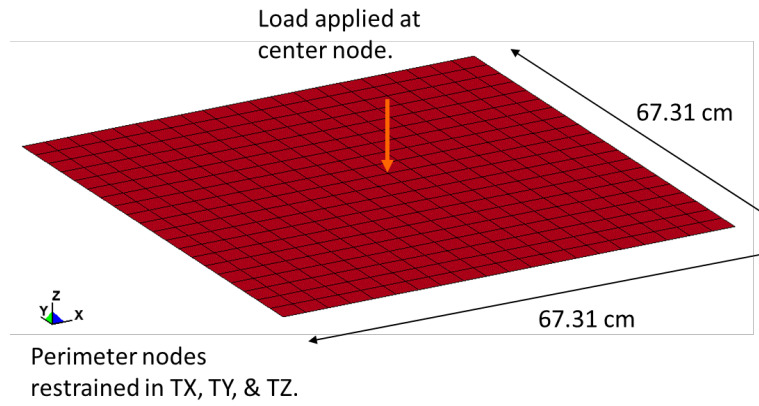


Figure 12. Schematic of Simple Model.

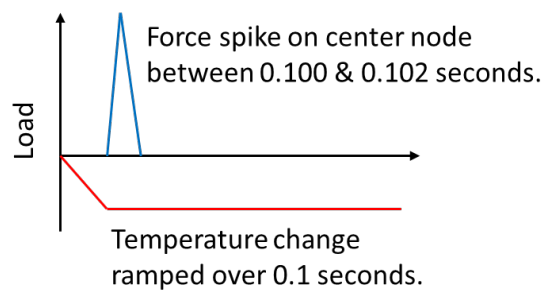


Figure 13. Loads for Simple Model (not to scale).

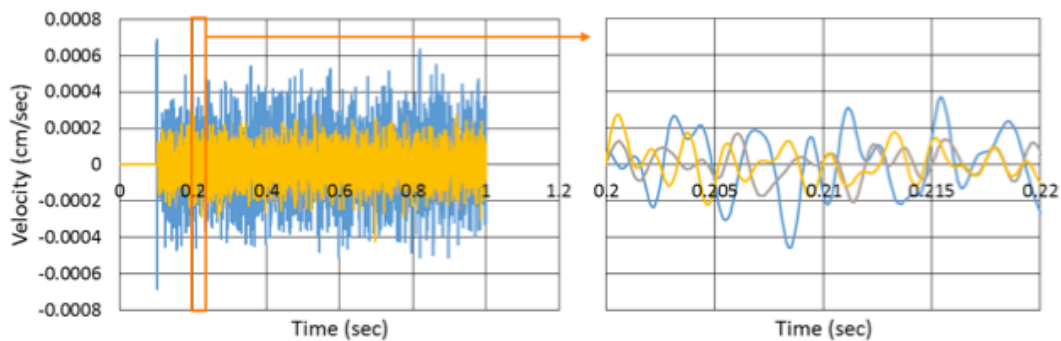


Figure 14. Sample velocity histories.

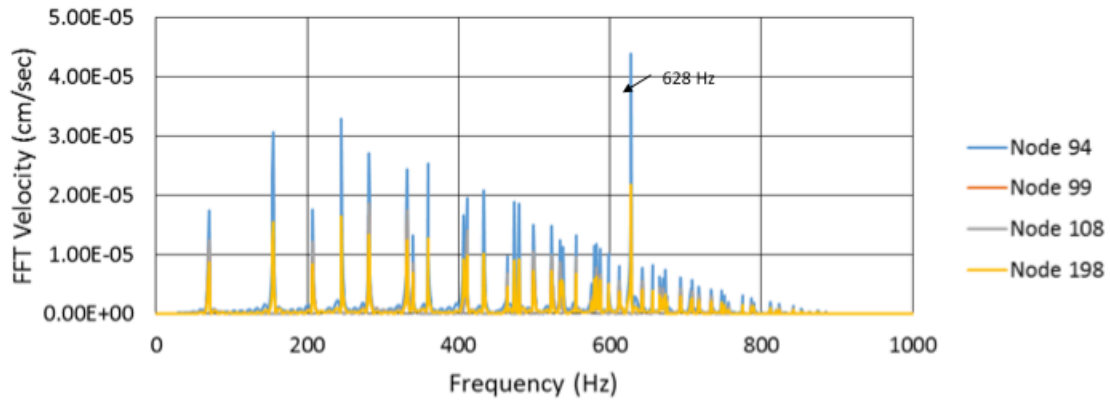


Figure 15. Fast Fourier Transform of sample velocity histories.

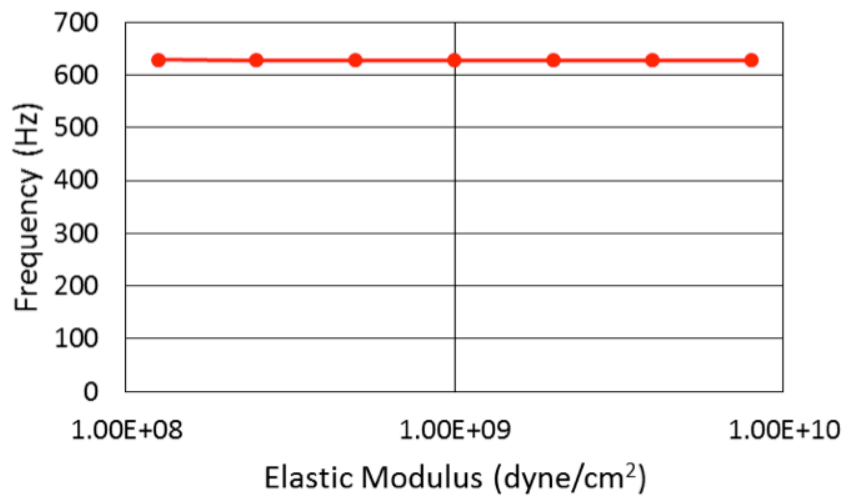


Figure 16. Frequency as a function of elastic modulus for the Simple Model.

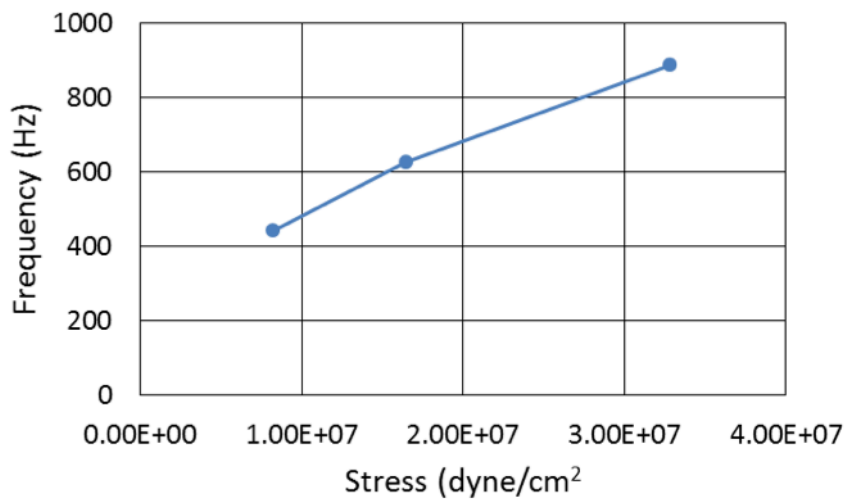


Figure 17. Frequency as a function of pretension for the Simple Model.

Small deflections do not significantly change the tension in the membrane. The deflection is resisted by the vertical component of the initial tension as the membrane deflects out of plane.

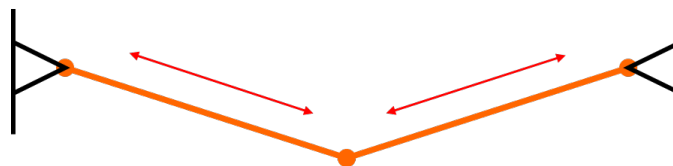


Figure 18. Mechanism for membrane's resistance to out-of-plane deflection.

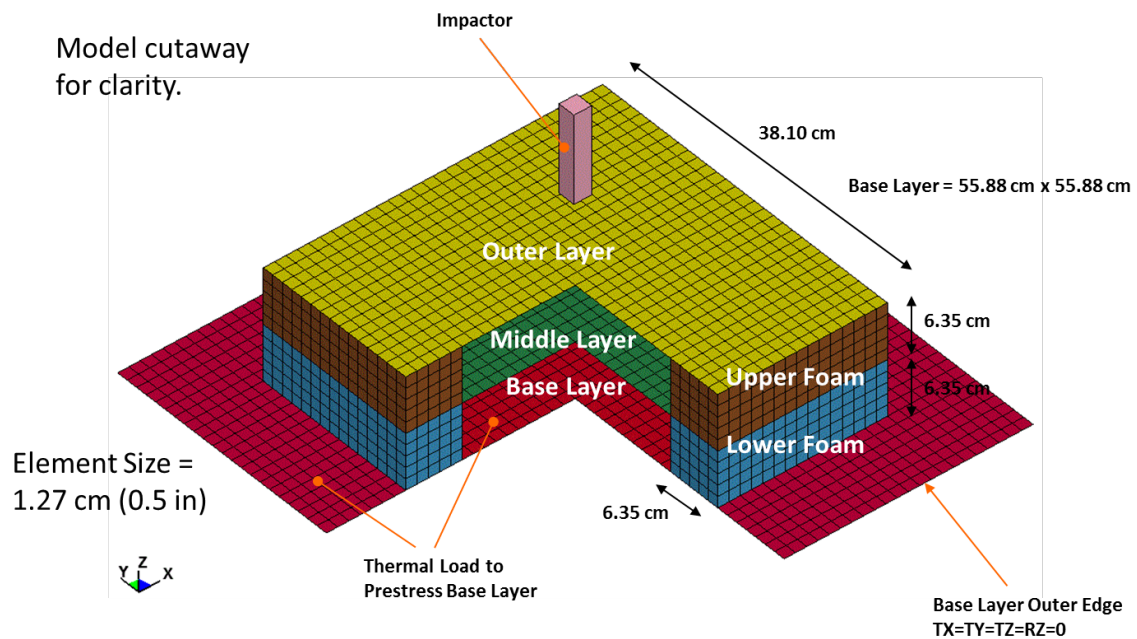


Figure 19. Layer Model

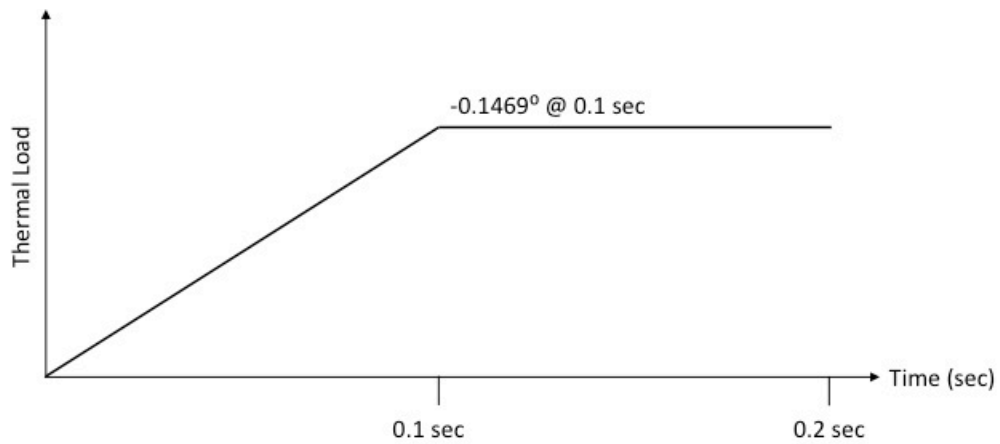


Figure 20. Pretension load for layer model.

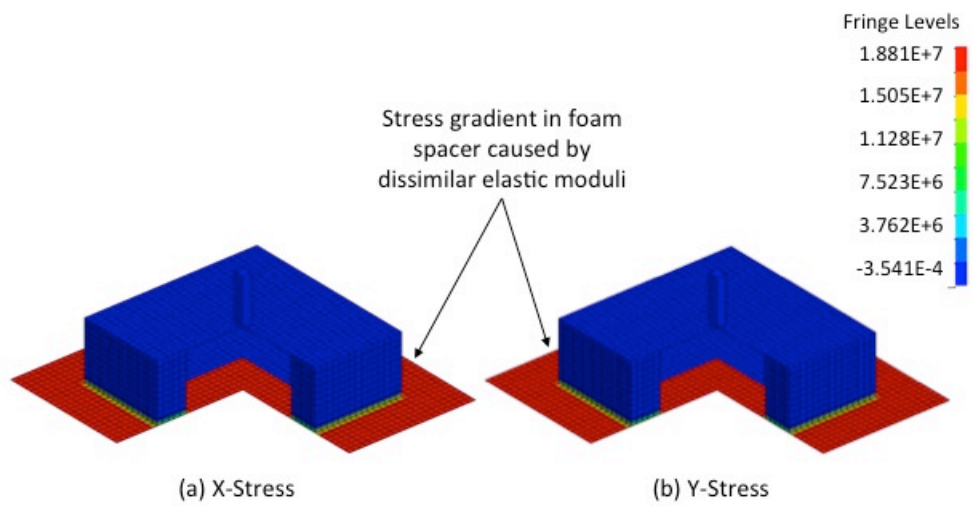


Figure 21. Restraint-layer pretension.

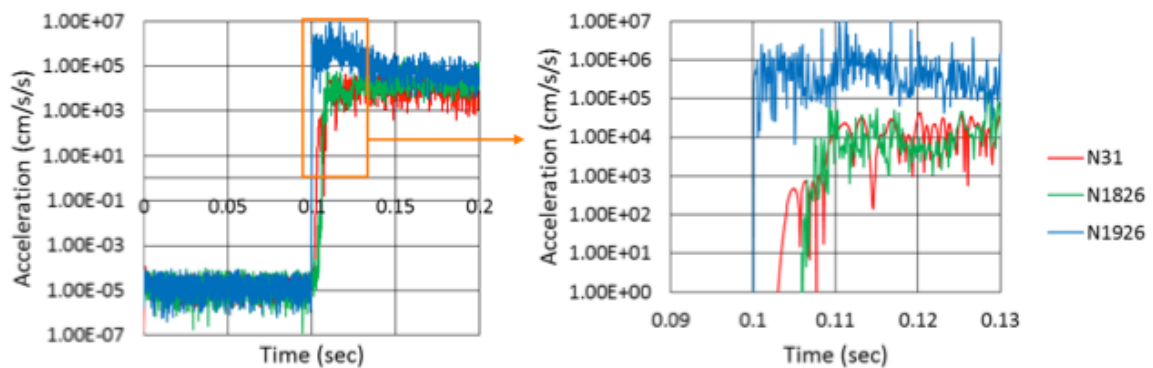


Figure 22. Sample Layer Model resultant acceleration responses.

REPORT DOCUMENTATION PAGE					Form Approved OMB No. 0704-0188	
<p>The public reporting burden for this collection of information is estimated to average 1 hour per response, including the time for reviewing instructions, searching existing data sources, gathering and maintaining the data needed, and completing and reviewing the collection of information. Send comments regarding this burden estimate or any other aspect of this collection of information, including suggestions for reducing this burden, to Department of Defense, Washington Headquarters Services, Directorate for Information Operations and Reports (0704-0188), 1215 Jefferson Davis Highway, Suite 1204, Arlington, VA 22202-4302. Respondents should be aware that notwithstanding any other provision of law, no person shall be subject to any penalty for failing to comply with a collection of information if it does not display a currently valid OMB control number.</p> <p>PLEASE DO NOT RETURN YOUR FORM TO THE ABOVE ADDRESS.</p>						
1. REPORT DATE (DD-MM-YYYY)		2. REPORT TYPE		3. DATES COVERED (From - To)		
01-11-2015		Technical Memorandum				
4. TITLE AND SUBTITLE Modeling of Local BEAM Structure for Evaluation of MMOD Impacts to Support Development of a Health Monitoring System				5a. CONTRACT NUMBER		
				5b. GRANT NUMBER		
				5c. PROGRAM ELEMENT NUMBER		
6. AUTHOR(S) Lyle, Karen H.; Vassilakos, Gregory J.				5d. PROJECT NUMBER		
				5e. TASK NUMBER		
				5f. WORK UNIT NUMBER 149030.01.99.99.99.23		
7. PERFORMING ORGANIZATION NAME(S) AND ADDRESS(ES) NASA Langley Research Center Hampton, VA 23681-2199				8. PERFORMING ORGANIZATION REPORT NUMBER L-20613		
9. SPONSORING/MONITORING AGENCY NAME(S) AND ADDRESS(ES) National Aeronautics and Space Administration Washington, DC 20546-0001				10. SPONSOR/MONITOR'S ACRONYM(S) NASA		
				11. SPONSOR/MONITOR'S REPORT NUMBER(S) NASA-TM-2015-218985		
12. DISTRIBUTION/AVAILABILITY STATEMENT Unclassified - Unlimited Subject Category 18 Availability: NASA STI Program (757) 864-9658						
13. SUPPLEMENTARY NOTES						
14. ABSTRACT This report summarizes initial modeling of the local response of the Bigelow Expandable Activity Module (BEAM) to micrometeorite and orbital debris (MMOD) impacts using a structural, non-linear, transient dynamic finite element code. Complementary test Results for a local BEAM structure are presented for both hammer and projectile impacts. Review of these data provided guidance for the transient dynamic model development. The local model is intended to support prediction using the global BEAM model, described in a companion report. Two types of local models were developed. One mimics the simplified Soft-Goods (fabric envelop) part of the BEAM NASTRAN model delivered by the project. The second investigates through-the-thickness modeling challenges for MMOD-type impacts. Both the testing and the analysis summaries contain lessons learned and areas for future efforts.						
15. SUBJECT TERMS Inflatable habitat; MMOD impacts; Numerical analysis						
16. SECURITY CLASSIFICATION OF:			17. LIMITATION OF ABSTRACT	18. NUMBER OF PAGES	19a. NAME OF RESPONSIBLE PERSON	
a. REPORT	b. ABSTRACT	c. THIS PAGE			STI Help Desk (email: help@sti.nasa.gov)	
U	U	U	UU	26	19b. TELEPHONE NUMBER (Include area code) (757) 864-9658	